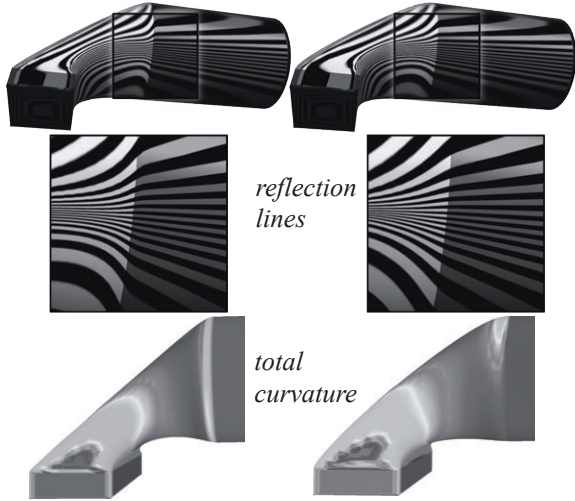


**Figure 11:** Hole filling: the half-sphere mesh was completed to close the “hole”. The left images show biharmonic reconstruction using region constraints and curve constraints with different prescribed tangents. The two rightmost images show the triharmonic reconstruction using region constraints and curve constraints with user-prescribed curvatures.



**Figure 12:** Blending between surfaces (cylinders with a square and circular cross-sections) using bi- and triharmonic equations and region boundary conditions. Note the smoother behavior of reflection lines in the triharmonic case.



**Figure 13:** Blending between two spherical caps, with controllable sharp features introduced using tangent conditions.

#### Acknowledgment

This work was supported in part by an NSF award IIS-0905502.

#### Appendix A: Ciarlet-Raviart discretization and region boundary conditions.

We outline the connection between solutions to the systems (12) and (10) here; a full rigorous treatment would require detailing assumptions on the smoothness spaces for boundary data and is beyond the scope of this paper. To simplify

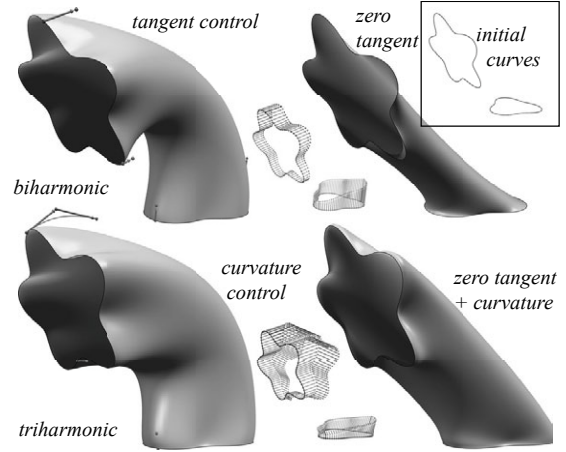


**Figure 14:** Filling in a patch between surfaces. Tangents or tangents+second derivatives can be specified at curves to obtain the desired shape.

consideration, we assume that the solutions are classical solutions, i.e.,  $\mathbf{u}$  is four times differentiable in  $\Omega$ . In this case, solutions of continuous problems with curve boundary conditions and region boundary conditions are identical, as long as the boundary conditions for the curve problem are sampled from  $\mathbf{u}^f$  for the region problem.

We consider a simplified situation with homogeneous Dirichlet conditions, i.e., we assume that for (10),  $\mathbf{u}^f = 0$ , and for (12),  $\mathbf{b}_0 = 0$  (this is a standard reduction for Dirichlet conditions, using substitution  $\mathbf{u} = \mathbf{u}^{orig} - \mathbf{u}^D$  where  $\mathbf{u}^D$  satisfies the Dirichlet condition [Bra02]). This reduction requires introducing a right-hand side for the second equation in the system:  $\Delta \mathbf{u} = \mathbf{v}$ ,  $\Delta \mathbf{v} = \Delta^2 \mathbf{u}^D = \mathbf{g}$ .

The Ciarlet-Raviart system (12) with lumped mass matrix with solution  $(\mathbf{v}_{\bar{\Omega}}^*, \mathbf{u}_{\bar{\Omega}}^*)$  can be rewritten in the form

$$\begin{bmatrix} -M^d & L_{\bar{\Omega}, \Omega} \\ L_{\Omega, \bar{\Omega}} & 0 \end{bmatrix} \begin{bmatrix} \mathbf{v}_{\bar{\Omega}} \\ \mathbf{u}_{\bar{\Omega}} \end{bmatrix} = \begin{bmatrix} -N_{\bar{\Omega}, 0}^{\partial \Omega} \mathbf{b}_1 - M_{\bar{\Omega}, 0}^{d, \Omega^c} \mathbf{v}_0^* \\ \mathbf{g}^{\Omega} \end{bmatrix}, \quad (16)$$

where we have subtracted  $M_{\bar{\Omega}, 0}^{d, \Omega^c} \mathbf{v}_0^*$  from both sides, to obtain the same left-hand side as in (10), and  $\mathbf{g}_j^{\Omega} = \langle \mathbf{g}, \varphi_j \rangle_{\Omega}$ . In comparison, the right-hand side of (10) is  $[0, \mathbf{g}^{\Omega_0}]$ , with  $\mathbf{g}_j^{\Omega_0} = \langle \mathbf{g}, \varphi_j \rangle_{\Omega_0}$ . As shown in [Sch78],  $(\mathbf{v}^*)^h$  converges to  $\mathbf{v}$  in  $L^2$ -norm, and  $\mathbf{v}$  is at least continuous on  $\bar{\Omega}$ . It can be extended by zero to all of  $\Omega_0$ , consistently with